INSTITUTE OF PHYSICS PUBLISHING NANOTECHNOLOGY
Nanotechnology **17** (2006) 4986–4990 doi:10.1088/0957-4484/17/19/035

Dielectrophoretic reconfiguration of nanowire interconnects

Alexander D Wissner-Gross

Department of Physics, Harvard University, 17 Oxford Street, Cambridge, MA 02138, USA

E-mail: alexwg@physics.harvard.edu

Received 13 July 2006
Published 15 September 2006
Online at stacks.iop.org/Nano/17/4986

Abstract
Silicon nanowire interconnects are dielectrophoretically assembled, reconfigured, and disassembled between gold electrodes in benzyl alcohol. Assembly of up to 55 μm long nanowires is demonstrated. Conductance enhancement is observed in the presence of single nanowires trapped between submerged electrodes. Phase inversion of electrode potentials allows the reversible reconfiguration of nanowires, either serially or in parallel. For disassembly, high-voltage bursts are observed to detonate trapped nanowires. The reconfiguration of colloidal electronic nanostructures opens up the possibility of nanostructured connection architectures for computation.

(Some figures in this article are in colour only in the electronic version)

M This article features online multimedia enhancements

1. Introduction

Programmability in electronic systems originates from the ability to form and reform nonvolatile connections. Devices in modern programmable architectures typically derive this ability from controlled internal changes in material composition or charge distribution [1]. However, for bottom-up nanoelectronic systems it may be advantageous to derive programmability not only from internal state, but also from the mechanical manipulation of mobile components. Proposed applications that require component mobility include neuromorphic networks of nanostructure-based artificial synapses [2], breadboards for rapid prototyping of nanodevice circuits [3, 4], and fault-tolerant logic in which broken subsystems are replaced automatically from a reservoir [5]. In this paper, we take the first step of demonstrating that interconnects, the simplest nanoelectronic components, can be assembled, reconfigured, and disassembled by an electromechanical process.

Various approaches for manipulating electronic nanostructures have been developed, including mechanical [6], optical [7, 8], electrostatic [9, 10], and dielectrophoretic [11] methods. Dielectrophoresis, in particular, is attractive for inexpensive and massively parallel manipulation [12] of neutral microscale and nanoscale objects using only standard semiconductor fabrication technologies. It has been used to trap a variety of structures from suspensions, including NiSi nanowires [13], CdS nanowires [14], GaN nanowires [15], carbon nanotubes [16], silicon microblocks [17], ZnO nanorods and nanobelts [18, 19], and gold nanowires [20]. Previous electrical transport measurements of dielectrophoretically trapped structures have been performed either after immobilizing the structures through drying [15, 17–19] or chemical binding [20], or performed over large films of parallel interconnects [16]. In this work we demonstrate for the first time that dielectrophoresis may also be used to reconfigure and disassemble nanowire interconnects and that our process is compatible with the assembly and electronic characterization of individual nanowire devices.

2. Experimental details

For interconnects, p-type silicon nanowires were grown by the vapour–liquid–solid method [21], using 20 nm Au nanocluster catalysts (Ted Pella), and SiH_4 reactant (99.7%) and B_2H_6 dopant (0.3%) in He carrier gas (100 ppm) at 450 Torr and 450 °C. Growth was performed for 10–60 min to achieve nanowire lengths of 10–60 μm. The nanowire growth wafer was sonicated lightly in isopropanol for 1 min. The suspension was vacuum filtered using a 12 μm mesh (Millipore Isopore) in order to remove unnucleated Au catalyst particles and short nanowires. The filter mesh was sonicated in isopropanol, and the suspension was again filtered. The second filter mesh was sonicated in benzyl alcohol for 2 min and the

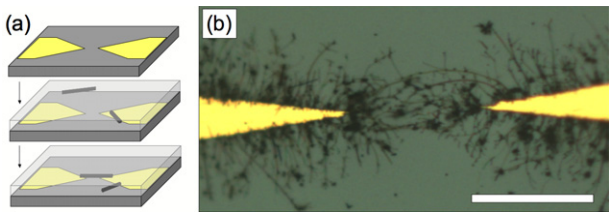

Figure 1. Dielectrophoretically trapped nanowires. (a) Schematic illustration of nanowire trapping process. (b) Light microscope image of multiple nanowires stably trapped between electrodes separated by 40 μm. The scale bar is 40 μm.

suspension was used for trapping experiments. Benzyl alcohol was selected as a viscous, low-vapour-pressure solvent [22] for reconfiguration in order to damp Brownian motion, minimize toxicity [23], and allow ambient operation. Additionally, its static relative permittivity is slightly smaller than that of bulk Si (11.9 versus 12.1, respectively) [22], reducing van der Waals interactions at low frequencies and favouring dielectrophoretic trapping of conductive structures [11]. Heavily doped silicon nanowires were selected as interconnects to demonstrate potential compatibility of our technique with the assembly of more complex semiconducting nanostructures, such as axial heterostructures [24].

Trapping experiments were performed with 100 nm Au electrodes (5 nm Cr wetting layer) to avoid oxidative damage, on a Si wafer with a 200 nm oxide to prevent shorts. Thicker electrodes, with reduced fringing fields, were found to better allow nanowires to migrate along their edges toward the trapping region. Thinner electrodes tended to permanently pin nanowires to the top electrode faces wherever they were first trapped. The electrodes were defined by e-beam lithography with a 10° taper angle and a 1 μm tip radius of curvature.

The nanowire suspension was pipetted onto the electrode chip to form a 250 μm thick reservoir, as shown schematically in figure 1(a). For trapping, electrode pairs were biased at 10 kHz to minimize both solvent electrolysis and parasitic capacitance. The bias was modulated into 10 ms bursts at 110 V_{RMS} with a period of 100 ms, which allowed migration of nanowires toward the trapping region in controlled steps. The time between bursts was manually increased to 1000 ms as nanowires approached the inter-electrode region, and the bursts were halted when the desired number of nanowires had been trapped. Movies of nanowire motion were recorded at 4 fps.

Electrical characterization was performed by manually switching the electrodes from the trapping voltage source to a measurement apparatus (Agilent 4156C). A 10 V sawtooth bias at 10 Hz was used and the measured currents were binned by voltage and averaged to remove hysteresis. Nanowire movement in the plane of the chip during transport measurement was minimal, since transport voltages were an order of magnitude smaller than trapping voltages.

3. Results and discussion

Confirmation that the trapping voltage was not substantially attenuated was provided by observation of a single scattering fringe around the electrodes in dark-field mode (supporting movie S1 is available at stacks.iop.org/Nano/17/4986, 1.4 MB MPEG), which was consistent with the 'DC' Kerr effect [11] at 155 V peak bias across a 10 μm gap. Nanowires up to 55 μm in length were stably trapped, as shown in figure 1(b), with noticeable bending due to the trapping field inhomogeneity. The longest previously reported one-dimensional nanostructures to be trapped by dielectrophoresis at both ends were less than 15 μm long, and showed minimal bending [14].

The burst method was also delicate enough to enable trapping of individual nanowires when the reservoir was diluted below 2×10^{-13} M, as shown in figure 2(a). Before the nanowire interconnects were assembled, the DC transport between electrode pairs was nearly ohmic, as shown in figure 2(b). The measured current of 0.3 μA at 1 V bias and 40 V s^{-1} sweep rate was consistent with electrooxidation of benzyl alcohol [25, 26] at 1 μm radius electrode tips. However, after a 50 μm long nanowire was trapped, the conductance became nonlinear and showed a 50% enhancement at 10 V bias, as shown in figure 2(c). Treating the device as an electrooxidative resistance in parallel with a series nanowire resistance and Schottky contacts [27], a nanowire transport curve was calculated, as shown in figure 2(d). The nanowire exhibited a calculated linear response resistivity of 3.8×10^{-3} Ω cm (6.0 MΩ resistance), consistent with a B doping ratio of 2000:1, and an estimated barrier potential of 2.0 V. The barrier potential was higher than the 0.34 V measured in evaporated Au/p-Si junctions [28], and is attributed to incomplete contact of the nanowire with the electrodes.

Further confirmation that dielectrophoretically trapped nanowires acted as interconnects was provided by substituting ethanol as a solvent and permitting the substrate to dry after trapping. A pair of nanowires thus trapped, as shown in figure 2(e), appeared to rest on both electrode faces but initial voltage sweeps yielded a 30 MΩ resistance, as shown in figure 2(f). After several sweeps, however, a sharp current turn-on was observed at 6.8–7.8 V, as shown in figure 2(g), which may indicate electrostatically induced bending of the nanowires to better contact the electrodes. Above the turn-on bias, the nanowires exhibited a 1.7 MΩ combined resistance, which is compatible with the solvent-based result.

The reported method for trapping nanowire interconnects furthermore enabled reconfiguration, since nanowires were maximally polarized when aligned between a pair of electrode tips. Reconfiguration of a nanowire bundle was achieved using 'source' and 'drain' electrodes with opposite phase and a 'latch' electrode with variable phase. Several nanowires were independently trapped between the source and latch electrodes with 100 ms period bursts, as shown in figure 3(a), and then bundled with 250 ms period bursts, as shown in figure 3(b). The phase of the latch electrode was then inverted, with the same burst period, causing the nanowire bundle to experience a dielectrophoretic force toward the drain electrode. Because the electrode tips were arranged in an isosceles right-triangle formation, the torque about the latch electrode was higher than that about the source electrode, and the nanowire remained in contact with the latch electrode during the motion, as shown in figure 3(c). The reconfiguration was completed 0.25–0.75 s after the phase inversion, as shown in figure 3(d), and could be reversed by restoring the original phase of the latch electrode, as shown in figure 3(e). Similarly, parallel reconfiguration of a pair of nanowire interconnects

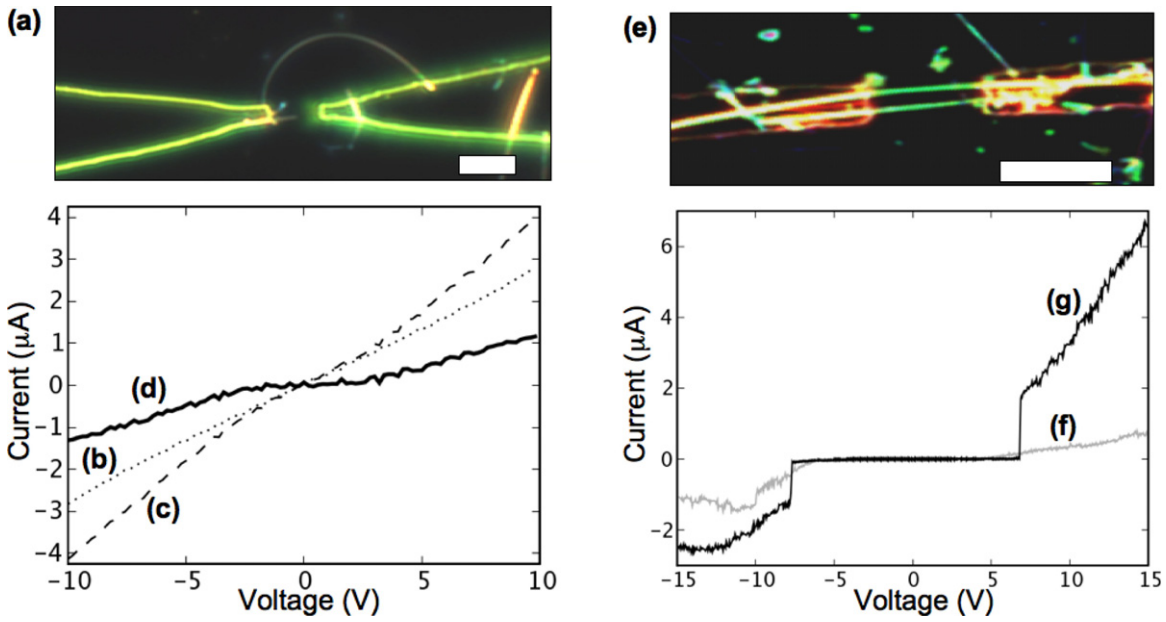

Figure 2. Electrical transport in trapped nanowires. (a) Dark-field microscope image of a single nanowire trapped by an electrode pair under solvent with electrical transport, (b) measured with solvent, (c) measured with trapped nanowire in solvent, and (d) calculated for nanowire alone. (e) Dark-field microscope image of two trapped nanowires on dried substrate with electrical transport measured (f) immediately after drying and (g) after several voltage sweeps. The scale bars are 10 μm.

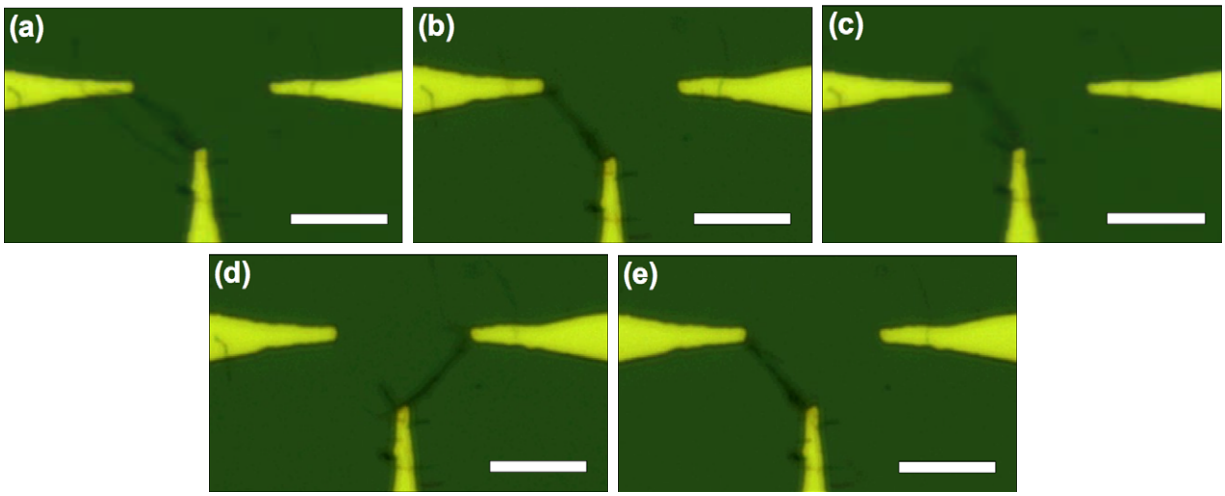

Figure 3. Microscope images of three-electrode serial reconfiguration of nanowires. The relative phase between the left (source) and middle (latch) electrodes is modulated from (a), (b) 180° to (c), (d) 0° to (e) 180°. The scale bars are 15 μm. Supporting movie S2 of this process is available at stacks.iop.org/Nano/17/4986 (0.5 MB MPEG).

was achieved with four electrodes in a 10 μm square, as shown in figure 4. To accomplish this, the relative phases between diagonally opposite electrodes were fixed and the relative phase of the diagonal pairs was inverted. Dielectric breakdown of some nanowires occurred and short fragments were visible around the connecting nanowires.

For theoretical comparison, we now calculate how rapidly a nanowire might be dielectrophoretically reconfigured. The dielectrophoretic force per unit length on a cylindrical nanowire with length l_{wire} and diameter d_{wire} is given by

$$F_{\text{dep}} = \tfrac{1}{8}\epsilon_{\text{solv}}\pi d_{\text{wire}}^2 \Re\left\{\vec{K}(f)\cdot\vec{\nabla}(\vec{E}^2)\right\}\hat{\nabla}(\vec{E}^2),$$

where ϵ_{solv} is the solvent permittivity and $\vec{K}(f)$ is the frequency-dependent Clausius–Mossotti factor [11]. For $l_{\text{wire}} \gg d_{\text{wire}}$, the Clausius–Mossotti component perpendicular to the nanowire axis is approximately

$$K_{\perp} = \frac{\tilde{\epsilon}_{\text{wire}} - \tilde{\epsilon}_{\text{solv}}}{\tilde{\epsilon}_{\text{solv}}(1-\frac{\pi}{8}) + \tilde{\epsilon}_{\text{wire}}(\frac{\pi}{8})},$$

where $\tilde{\epsilon}_{\text{X}} \equiv \epsilon_{\text{X}} - \text{i}\sigma_{\text{X}}/(2\pi f)$ are the complex permittivities of nanowire and solvent (the solvent is assumed to be non-conductive at trapping frequencies). Approximating the gradient of the field energy density in the inter-electrode space as uniform, $\nabla(\vec{E}^2) \sim V_{\text{sd}}^2/L^3$, where L is the distance between electrode tips.

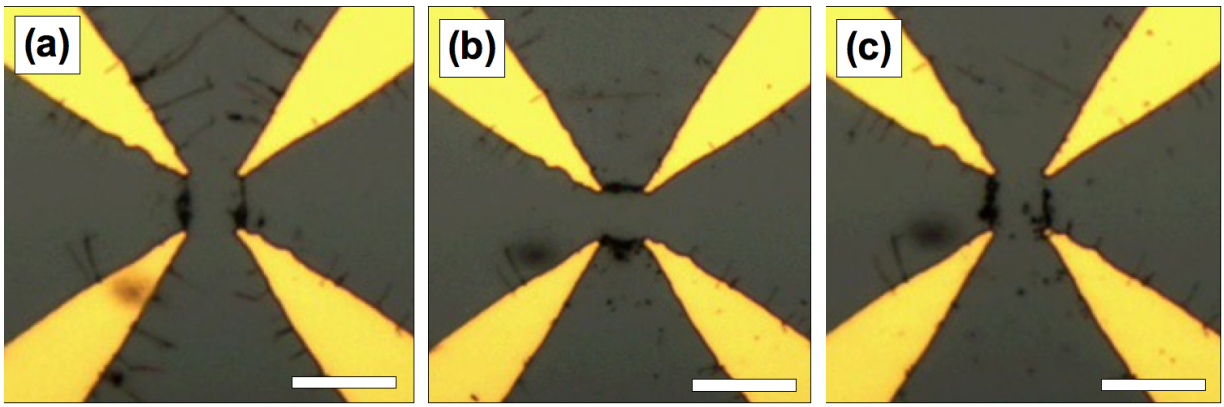

Figure 4. Microscope images of four-electrode parallel reconfiguration of nanowires. Each pair of diagonally opposite electrodes is held at a constant relative phase of 180°, while the relative phase between the upper-left and upper-right electrodes is modulated from (a) 0° to (b) 180° to (c) 0°. The scale bars are 20 μm. Supporting movie S3 of this process is available at stacks.iop.org/Nano/17/4986 (2.4 MB MPEG).

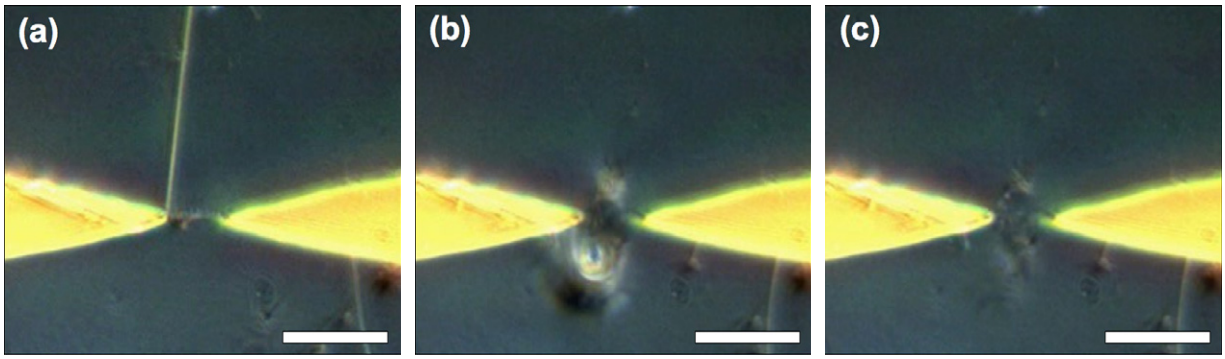

Figure 5. Disassembly of nanowire interconnects by thermal detonation. (a) Stably trapped nanowire before detonating voltage pulse. (b) Vapour bubble resulting from thermal detonation. (c) Only sub-micron fragments remain. The scale bars are 20 μm. Supporting movie S4 of this process is available at stacks.iop.org/Nano/17/4986 (2.1 MB MPEG).

The dielectrophoretic force is opposed by Stokes drag. The drag coefficient for an infinitely long, cylindrical nanowire [29] is given by

$$C_{\mathrm{D}} \equiv \frac{F_{\mathrm{drag}}}{\frac{1}{2}\rho_{\mathrm{wire}} u^2 d} \approx \frac{8\pi}{Re\,(2.002 - \ln Re)},$$

where F_{drag} is the drag force per unit length, ρ_{wire} is the nanowire density, u is the nanowire velocity, and $Re \sim d\rho_{\mathrm{solv}} u/\mu$ is the Reynolds number for solvent density ρ_{solv} and dynamic viscosity μ. Assuming bulk mechanical properties of silicon and benzyl alcohol [22] and matching drag and dielectrophoretic forces, the terminal velocity during switching perpendicular to the nanowire axis is calculated to be $u_{\perp} \approx 30\ \mu\mathrm{m\ s}^{-1}$, implying a 0.3 s reconfiguration time. This time is consistent with the serial reconfigurations observed, validating our model.

Finally, it should be mentioned that electrically driven nanowire disassembly was also found to occur. In an example of this effect, a single nanowire that was initially trapped on one electrode, as shown in figure 5(a), was pulled into the inter-electrode region and a gas bubble immediately formed there, as shown in figure 5(b). After the bubble dispersed, only short nanowire fragments remained, as shown in figure 5(c). This effect was observed for about 1/3 of the nanowires trapped in inter-electrode regions and might be explained by variation in the nanowire conductivities and/or the formation of exceptionally good contacts, which could lead to current densities as high as 5×10^{10} A m^{-2} and thermal detonation. After the original nanowires were destroyed, the inter-electrode regions were typically able to trap new interconnects, so this effect might prove useful in fault-tolerant applications for severing connections to non-functioning components.

4. Conclusions

The first assembly, reconfiguration, and disassembly of nanowire interconnects through dielectrophoresis has been demonstrated. Silicon nanowires up to 55 μm long were trapped, and solvent-based transport studies show a 50% conductivity enhancement in the presence of the nanowires. Once assembled, these nanowire interconnects could then be reconfigured and disassembled using periodic voltage bursts. These results open up the possibility of colloidal, nanostructured connection architectures for computation.

Acknowledgments

The author is especially grateful to C M Lieber for his generous guidance and support, and for use of his laboratory, and to

F Patolsky for very helpful discussions. The author also thanks the Fannie and John Hertz Foundation for doctoral funding. This work made use of Harvard Center for Nanoscale Systems and NSF/NNIN facilities. This material was supported in part by the United States Air Force and DARPA under Contract No. FA8750-05-C-0011. Any opinions expressed are those of the author and do not necessarily reflect the views of the United States Air Force or DARPA.

References

[1] Rose J, el Gamal A and Sangiovanni-Vincentelli A 1993 *Proc. IEEE* **81** 1013
[2] Türel Ö and Likharev K 2003 *J. Circ. Theor. Appl.* **31** 37
[3] Ellenbogen J C and Love J C 2000 *Proc. IEEE* **88** 386
[4] Moser J, Panepucci R, Huang Z P, Li W Z, Ren Z F, Usheva A and Naughton M J 2003 *J. Vac. Sci. Technol.* B **21** 1004
[5] Lala P K 2001 *Self-Checking and Fault-Tolerant Digital Design* (San Diego, CA: Academic) p 172
[6] Huang Y, Duan X, Wei Q and Lieber C M 2001 *Science* **291** 630
[7] Agarwal R, Ladavac K, Roichman Y, Yu G, Lieber C M and Grier D G 2005 *Opt. Express* **13** 8906
[8] Pauzauskie P J, Radenovic A, Trepagnier E, Shroff H, Yang P and Liphardt J 2006 *Nat. Mater.* **5** 97
[9] Jang J E, Cha S N, Choi Y, Amaratunga G A J, Kang D J, Hasko D G, Jung J E and Kim J M 2005 *Appl. Phys. Lett.* **87** 163114
[10] Rueckes T, Kim K, Joselevich E, Tseng G Y, Cheung C L and Lieber C M 2000 *Science* **289** 94
[11] Pohl H A 1978 *Dielectrophoresis* (Cambridge: Cambridge University Press)
[12] Chiou P Y, Ohta A T and Wu M C 2005 *Nature* **436** 370
[13] Dong L, Bush J, Chirayos V, Solanki R, Jiao J, Ono Y, Conley J F Jr and Ulrich B R 2005 *Nano Lett.* **5** 2112
[14] Duan X, Huang Y, Cui Y, Wang J and Lieber C M 2001 *Nature* **409** 66
[15] Kim T H, Lee S Y, Cho N K, Seong H K, Choi H J, Jung S W and Lee S K 2006 *Nanotechnology* **17** 3394
[16] Chen Z, Yang Y, Chen F, Qing Q, Wu Z and Liu Z 2005 *J. Phys. Chem.* B **109** 11420
[17] Lee S W and Bashir R 2003 *Appl. Phys. Lett.* **83** 3833
[18] Harnack O, Pacholski C, Weller H, Yasuda A and Wessels J M 2003 *Nano Lett.* **3** 1097
[19] Lao C S, Liu J, Gao P, Zhang L, Davidovic D, Tummala R and Wang Z L 2006 *Nano Lett.* **6** 263
[20] Shang L, Clare T L, Eriksson M A, Marcus M S, Metz K M and Hamers R J 2005 *Nanotechnology* **16** 2846
[21] Cui Y, Lauhon L J, Gudiksen M S, Wang J and Lieber C M 2001 *Appl. Phys. Lett.* **78** 2214
[22] Lide D R (ed) 2001 *CRC Handbook of Chemistry and Physics* 82nd edn (New York: CRC Press) pp 3–52 , 6–163, 12–59
[23] Nair B 2001 *J. Toxicol.* **20 S3** 23
[24] Gudiksen M S, Lauhon L J, Wang J, Smith D and Lieber C M 2002 *Nature* **415** 617
[25] Mayeda E A, Miller L L and Wolf J F 1972 *J. Am. Chem. Soc.* **94** 6812
[26] Kishioka S Y, Umeda M and Yamada A 2003 *Proc. Electrochem. Soc. Mtg (Paris)* Abstract No. 2474
[27] Fuhrer M S, Lim A K L, Shih L, Varadarajan U, Zettl A and McEuen P L 2000 *Physica* E **6** 868
[28] Smith B L and Rhoderic E H 1971 *Solid-State Electron.* **14** 71
[29] Tritton D J 1988 *Physical Fluid Dynamics* (Oxford: Oxford University Press) p 32